



The Effect of Sm_2O_3 on the Sintering and Grain Growth Behaviors of SnO_2 -Based Ceramics

Hajieh Bastami ^{a,d*}, Ehsan Taheri-Nassaj ^b, Philippe F. Smet ^{c,d}, Dirk Poelman ^{c,d}

^a Technical and Vocational University of Tehran, Faculty of Material Science and Engineering, Shariaty College, 18918-16851, Tehran, Iran

^b Department of Materials Science and Engineering, Tarbiat Modares University, Tehran, Iran

^c LumiLab, Department of Solid State Sciences, Ghent University, Krijgslaan 281/S1, B-9000 Ghent, Belgium

^d Center for Nano and Biophotonics (NB Photonics), Ghent University, Ghent, Belgium

PAPER INFO

Paper history:

Received 30 June 2019
Accepted in revised form 3 September 2019

Keywords:

Samarium Oxide
Tin Oxide
Rare Earth
Segregation
Sintering
Nanosized Materials

ABSTRACT

The effect of samarium oxide was examined on the sintering, microstructure, and grain growth behaviors of (Co, Nb)-doped SnO_2 -based ceramics prepared by co-precipitation method. The sintered samples were studied through x-ray diffraction (XRD), scanning electron microscopy (SEM), and electron dispersive spectroscopy (EDS) analyses. The microstructure observations revealed that the samples were near fully dense at a sintering temperature of 1200°C for 1h. The samarium doping prevented accelerated grain growth of the SnO_2 -based ceramic in the final stage of the sintering. The mean grain size of the SnO_2 -based ceramic without Sm_2O_3 doping was 2.70 μm , which was reduced to 0.887 μm for the sample doped with 0.05mol% Sm_2O_3 . The grain size reduction of samples doped with Sm_2O_3 could be attributed to the segregation of Sm_2O_3 at the grain boundaries.

1. INTRODUCTION

Recently, many papers have been devoted to the synthesis and sintering of nanocrystalline ceramics due to the significant improvement in their properties as compared with the conventional coarse grain compacts [1-6]. Nanosized powders have a high surface area that can be applied to decrease the sintering temperature, increase the density after firing, and produce a small grain size in the fired ceramics [4-6]. The co-precipitation is a simple method to prepare homogenous nanostructured powders [1].

Tin oxide is an n-type semiconductor with a tetragonal structure, which has many interesting electronic properties. Pianaro et al. (1995) found (Co, Nb)-doped SnO_2 -based ceramics as new promising varistor devices [7]. Cerri et al. studied the sintering behavior of CoO-doped SnO_2 -based ceramics. They reported that the sintering of this system is controlled by

diffusion in the solid-state. Addition of cobalt oxide leads to the creation of additional vacancies, which increases the diffusion rate of oxygen ions, resulting in high values of densities ($\geq 99\%$ of theoretical density) in SnO_2 -based ceramics [8]. Addition of Cr_2O_3 [7, 9, 10] or rare earth oxides such as Gd_2O_3 [11], Yb_2O_3 [12], La_2O_3 , Pr_2O_3 [13,14], Dy_2O_3 [15], and Sm_2O_3 [4,16] to (Co, Nb)-doped SnO_2 -based varistors improves the non-linear electrical properties of this system. The lanthanide ions that are segregated at the grain boundary are the origin of potential barriers [17]. The role of dopants has been observed on the grain growth behavior in other ceramic systems such as MgO-doped Al_2O_3 [18], Sm_2O_3 -doped CeO_2 [19], and Y_2O_3 -doped CeO_2 [20]. The segregation of dopants elements at the grain boundaries prevents the grain growth of these ceramic oxides [10-21]. The densification process consists of solid particle bonding

*Corresponding Author Email: Hbastami@tvu.ac.ir,
Hajiehbastami@gmail.com (H. Bastami)

or neck formation followed by the continuous closing of pores from a largely open porosity to essentially a pore-free body. The solid-state densification is considered accomplished through three stage [4, 21, 23-26] including initial, intermediate, and final. The classical sintering theory describes the multiple mechanisms involved throughout the mentioned three stages as evaporation-condensation, surface diffusion, grain boundary diffusion, bulk diffusion, and plastic deformation. There is no systematic study on the sintering and grain growth behaviors of SnO₂-based ceramics prepared by nanosized powders.

The influence of Sm₂O₃ on the electrical properties of SnO₂-based varistors was already addressed [16]. In this research, the effect of Sm₂O₃ on the sintering, microstructure development, and grain growth of (Co, Nb)-doped SnO₂-based ceramics was studied at various temperatures. Furthermore, the effect of samarium on the different stages of sintering of SnO₂-based ceramics has been investigated for the first time.

2. EXPERIMENTAL PROCEDURES

2.1. Powder Synthesis and Characterization

The nanosized doped-SnO₂ powder was synthesized using the co-precipitation method. The analytical grades of SnCl₄.5H₂O (Riedel), Sm(NO₃)₃.6H₂O (Alfa Aesar), Co(NO₃)₂.6H₂O (BDH), and NbCl₅ (Merck) were employed. Initially, two solutions (the first one containing SnCl₄.5H₂O and the second one containing the dopant cations) were prepared. Nitric acid (HNO₃) was added to the solution containing Sm(NO₃)₃.6H₂O, Co(NO₃)₂.6H₂O, and NbCl₅. The prepared solution was added to the solution containing SnCl₄.5H₂O to increase the solution pH. The system was stirred continuously for 24h. The precipitates were then filtered and washed with deionized water. The dried powder was then calcined at 700°C [1].

The samples were given the following specific names of SCN: 98.95 SnO₂+ 1.00 CoO+0.05 Nb₂O₅ (mol%) and SCNSm: 98.90 SnO₂+ 1.00 CoO+0.05 Nb₂O₅+0.05 Sm₂O₃ (mol%) for identification.

2.2. Compaction, Sintering, and Microstructure Observation

The samples were prepared in the way that the synthesized powders were first wet milled in ethanol using zirconia balls for 1h. The obtained powders were granulated with PVA binder and then, uniaxially pressed (15MPa) into discs with 20.0mm diameter and 1.0mm thickness followed by cold isostatic pressing (CIP) (240MPa) after drying at 60°C. The discs were placed in a zirconia crucible and fully surrounded with the powders of matching compositions to avoid cobalt loss during the sintering and to ensure the desired compositions after burning out the PVA binder at 650°C. The discs were sintered by conventional

method at 800°C, 900°C, 1000°C, 1100°C, and 1200°C for 1h in air, and then, cooled down freely to the ambient temperature.

The apparent density of the sintered samples was estimated through the Archimedes method. The crystal structure of the ceramics was characterized by X-ray diffraction (XRD) with Cu K α radiation (Philips X-pert). The grain size was calculated using the Mendelson Equation [22].

3. RESULTS AND DISCUSSION

3.1. Powder Characterization

The XRD pattern of SCNSm sample calcined at 700°C for 2h displayed only tetragonal rutile (not shown) [1]. Figure 1 shows the SEM micrograph for SCNSm. The sizes of the particles were in the range of 45-70nm, which were spherical in shape.

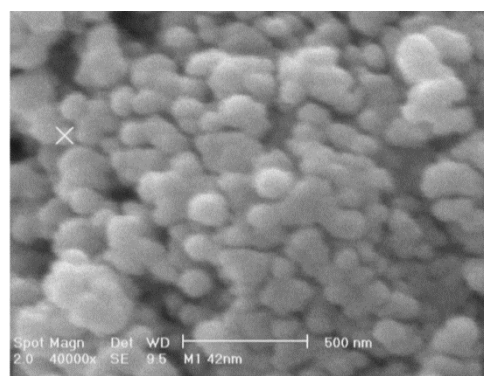


Figure 1. The SEM micrograph of the sample SCNSm doped with 0.05mol% Sm₂O₃ calcined at 700°C for 2h

3.2. Densification Behavior of the Nanosized Powder

The XRD pattern of SCNSm sintered at 1200°C for 1h confirmed the pure tetragonal rutile structure of SnO₂ (Fig. 2).

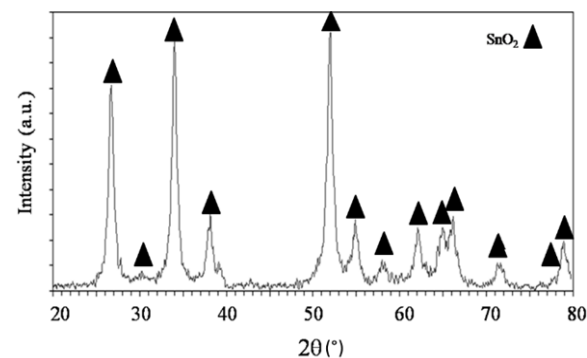


Figure 2. The XRD pattern of SCNSm sintered at 1200°C for 1h, revealing only the tetragonal structure of SnO₂

The SEM micrographs of SCN and SCNSm sintered at various temperatures are shown in Fig. 3. As clearly shown, the difference between SCN and SCNSm was considerable. The addition of Sm_2O_3 reduced the mean grain size of (Co, Nb)-doped SnO_2 and prevented the grain growth at the temperatures of 1000°C , 1100°C , and 1200°C , which is consistent with the findings of Li et al. in Sm_2O_3 -doped CeO_2 [19].

Fig. 4 shows the effect of sintering temperature on the relative density and grain size of SCN and SCNSm samples. The density versus temperature graphs exhibits a sigmoidal shape for both SCN and SCNSm. No significant densification was observed below 900°C . The relative density for both SCN and SCNSm samples sintered at 900°C was 65% of the theoretical density [7]. The SEM micrographs of fracture of these samples are shown in Figs. 3a and 3b. The surface diffusion is considered as the principle mechanism during the initial stage. The intermediate stage normally covers the major part of the sintering process (the relative density between ~65 and 90% of the theoretical density) and ends when the density is ~90% of the theoretical density [24-26]. As shown in Fig. 4, the relative densities of SCN and SCNSm samples were about 83% of the theoretical density (Fig. 4a) and 78% of the theoretical density (Fig. 4b), respectively. The mean grain sizes of SCN and SCNSm sintered at 1000°C were as much as 290nm (Fig. 4c) and 140nm (Fig. 4d), respectively. The mean grain size did not show a remarkable change through the intermediate stage of sintering (see the fractured surfaces of these samples in Fig. 3c and 3d). Increasing in sintering temperature up to 1200°C caused a full density in the samples (>99% of the theoretical density) [24-26]. The high-density values of both SCN and SCNSm indicated that the cobalt oxide efficiently promoted the densification of SnO_2 , as described by solid-state sintering. The mean grain sizes of SCN and SCNSm samples sintered at 1200°C were $2.70\mu\text{m}$ and $0.887\mu\text{m}$, respectively. Fig. 3g and

3h confirm the reduction of the grain size upon Sm_2O_3 doping.

Fig. 3g and 3h confirm the high density of samples without and doped with Sm_2O_3 . The relative density of SCN and SCNSm samples were 99.90% and 99.41% of the theoretical density, respectively. The high values of density of the SnO_2 ceramics (>99% of the theoretical density) were mainly a result from the relatively low sintering temperature of nanopowders (1200°C) compared with the usual sintering temperature of $1300\text{-}1400^\circ\text{C}$ [7-15]. Thus, the addition of Sm_2O_3 prevents the grain growth of SnO_2 grains by segregation at the grain boundaries and formation of some samarium compounds [4].

The mean grain size of SCN and SCNSm samples as a function of the relative density for different temperatures are shown for SCN and SCNSm in Fig. 5. The grain size of SCN and SCNSm samples increases by increasing the temperature. The relative density of SCN was higher than SCNSm in the intermediate stage of sintering. As shown in Fig. 5, the retardation effect of samarium doping was observed on densification in the intermediate stage, which is consistent with the findings of Li et al. in Sm_2O_3 -doped CeO_2 [19]. Moreover, fast grain growth of SCN occurred as the relative density exceeded 90% of the theoretical density (Fig. 5), which is consistent with the findings of Hesabi et al. for $8\text{Y}_2\text{O}_3$ stabilized ZrO_2 [27]. The accelerated grain growth in polycrystals is also reckoned to always accompany the final stage during the sintering. It has been confirmed that open pores, referring to the intermediate stage of sintering, collapse to form closed ones after the final stage starts. Such a collapse results in a substantial decrease in pore pinning, which triggers accelerated grain growth [1,18-21]. As shown in Fig. 5, the samarium doping prevented accelerated grain growth in the final stage of sintering. Therefore, the samarium doping provides a homogenous microstructure that is necessary to obtain the desired electrical, mechanical, and optical properties.

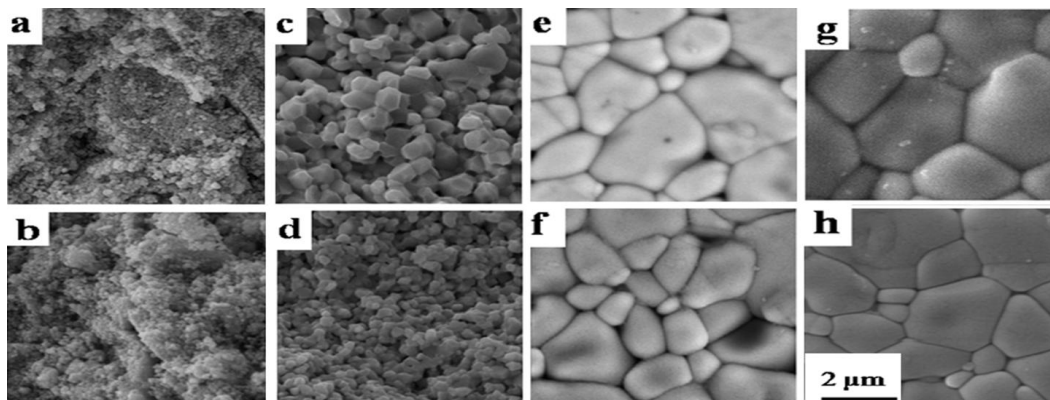


Figure 3. The SEM micrographs of the samples without and doped with 0.05mol% Sm_2O_3 sintered at temperatures of 900°C (a,b), 1000°C (c,d), 1100°C (e,f), and 1200°C (g,h) for 1h

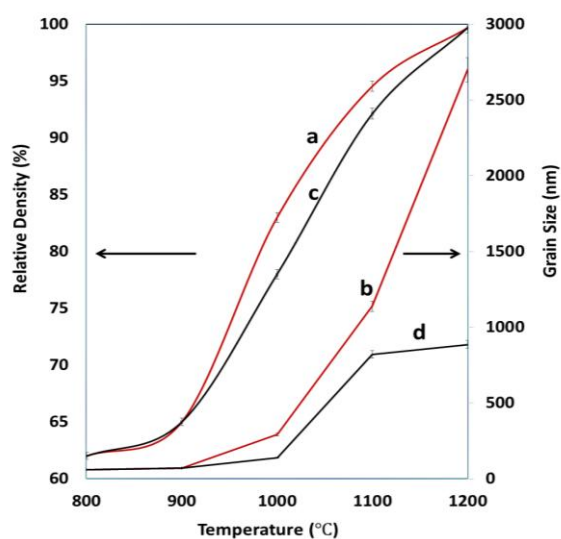


Figure 4. The plots of variations in relative density and grain size of undoped SnO₂ with temperature (a and c), and the corresponding plots for the sample doped with 0.05mol% Sm₂O₃ (b and d)

Fig. 6 shows the SEM and EDS analyses for the sample doped with 0.05 Sm₂O₃ (mol%) in different points including the grain (point A) and the grain boundary (point B). The weight percent ratios of Sn, Nb, Co, and Sm are given in Fig. 6. As clearly shown in Fig. 6, the microstructure of ceramics sintered at 1200°C contained only SnO₂ phase. The EDS results confirmed that the grains were predominantly composed of SnO₂ and the grain boundary was Sm rich, similar to the findings of other studies [4,7-15]. The higher amounts of Co and Sm in the point B (grain boundary) in the comparison with the point A (grain) could be related to the segregation of cobalt and samarium at the grain boundary.

As reported in the earlier work, the absence of any glass phase in the STEM image confirmed the formation of a solid solution [4]. Therefore, the sintering process is controlled by the solid-state mechanism. Sm atoms were segregated at some grain boundaries and formed Sm-rich regions. Moreover, Co atoms segregated at some triple points and formed some Co-rich regions [4].

The samarium doping retarded both densification and grain growth of the SnO₂-based ceramics. Kingery completely interpreted the ceramic grain boundary phenomena such as solute segregation, grain boundary diffusion, structure, and electrostatic potential [19]. It was reported in this research that the major driving forces leading to the segregation of equilibrium concentration of solute at the grain boundary are the electrostatic potential of interaction between the solute and the charged grain boundary. Trivalent cations

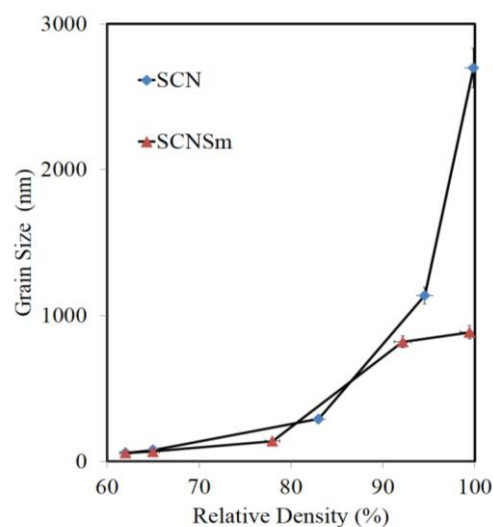
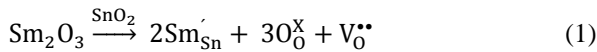


Figure 5. The mean grain size as a function of the relative density for undoped SnO₂ sample and the one doped with 0.05mol% Sm₂O₃, sintered at 800°C, 900°C, 1000°C, 1100°C, and 1200°C for 1h

possess an effective negative charge compared to host cations. They tend to enrich at grain boundaries due to the space charge effect [19]. In many solid solutions, solute atoms are known to segregate at the boundary forming a solute cloud in the vicinity of the boundary. Li et al. reported that the excess samarium cations located at grain boundary generate a steep concentration gradient between the grain interior and the grain boundaries, giving a strong drag to grain boundary migration resulting in an effective retardation of grain growth during the sintering as well as in the fully densified bodies of Sm₂O₃-doped CeO₂-based ceramics [19]. The solute segregation occurs when there are lower energy sites at the grain boundary for the solute atoms than in the bulk. When the grain boundary migrates, the solute atoms segregated at the grain boundary are apt to remain attached to the grain boundary that provides them with low energy sites. In other words, the solutes tend to diffuse along with the moving boundary, which acts as a drag force against the boundary movement [25]. The concentration of the solute atoms, segregated at the grain boundary, is higher than in the bulk of the grain, but a solid solution still exists. Similar to the Sm₂O₃-doped-CeO₂-based ceramics, the inhibition of the grain growth of SnO₂-based ceramics by Sm₂O₃ is believed to occur by a mechanism of solute drag [19]. The concentration of the solute (dopant) is often believed to be well below the solid solubility limit in ceramics, which is not clear in some systems. It has been found that the effectiveness of the dopant in suppressing grain growth depends on its ability to

segregate at the grain boundary [25-28]. A second factor leading to boundary segregation is the reduction in the elastic strain energy of the crystal lattice due to the size difference between the solute atoms and the host atoms for which it substitutes [21,25]. Since the ionic radius of Sm^{3+} (0.096nm) is larger than Sn^{4+} (0.071nm), the substitution of Sn^{4+} by Sm^{3+} leads to the distortion of SnO_2 lattice [4,16] as:



The inhibition of grain growth through the addition of Sm_2O_3 could be related to the strain energy caused by lattice distortion. Therefore, the samarium doping retarded both densification and grain growth of the SnO_2 -based ceramics in the intermediate stage of sintering and prevented the grain growth in the final stage.

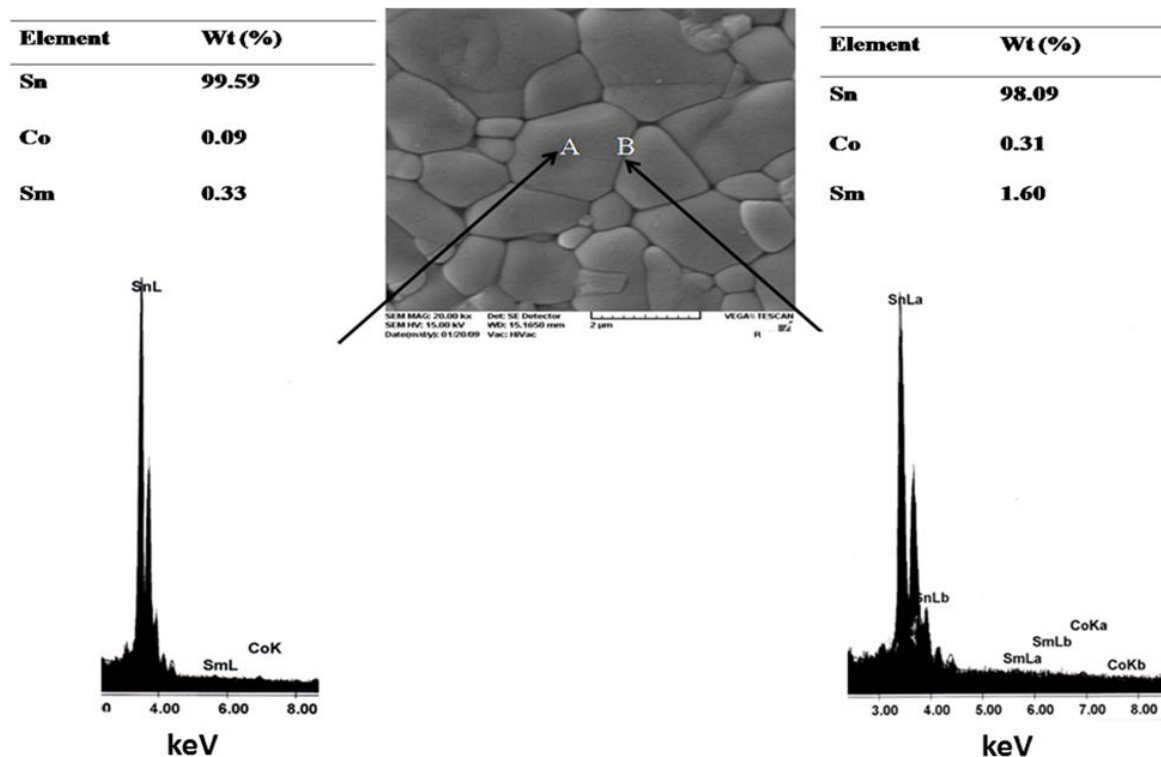


Figure 6. The energy dispersive spectra (EDS) analysis for the sample doped with 0.50 Sm_2O_3 (mol%): the grain (point A) and the grain boundary (point B)

4. CONCLUSIONS

In the present work, the effect of Sm_2O_3 was investigated on the sintering and grain growth behaviors of (Co, Nb)-doped SnO_2 -based ceramics prepared by co-precipitation method and the following results were obtained:

(1) The high densities of the sintered SnO_2 ceramics (>99%TD) are mainly benefited from the relatively low sintering temperature (1200°C), which is a direct result of the good dispersion and the ultrafine particle size of the nanostructured SnO_2 powders prepared by chemical route.

- (2) The samarium doping also prevented accelerated grain growth in the final stage of sintering. The mean grain size of the SnO_2 -based ceramics without Sm_2O_3 doping was 2.70 μm . This value was reduced to 0.877 μm by doping of 0.05mol% Sm_2O_3 .
- (3) The grain size reduction could be attributed to the segregation of Sm_2O_3 at the grain boundaries.

5. REFERENCES

- Bastami, H., Taheri-Nassaj, E., "Synthesis of nanosized (Co, Nb, Sm)-doped SnO_2 powders using co-precipitation meth", *Journal of Alloys and Compounds*, Vol. 495, No. 1, (2010), 121-125.

2. Hayati, R., Feizpour, M., Ebadzadeh, T., "Effect of nano and micron WO_3 on microstructure and electrical properties of lead free potassium sodium niobate piezoceramics", *Advanced Ceramic Progress*, Vol. 1, No. 3, (2015), 11-15.
3. Nikzad, L., Ghofrani, S., Majidianm H., Ebadzadeh, T., "Effect of ball milling on reactive microwave sintering of MgO-TiO_2 System", *Advanced Ceramic Progress*, Vol. 2, No. 3, (2016), 25-28.
4. Bastami, H., Taheri-Nassaj, E., Smet, P.F., Korthout, K., Poelman, D., "(Co, Nb, Sm)-doped tin dioxide varistor ceramics sintered using nanopowders prepared by coprecipitation method", *Journal of the American Ceramic Society*, Vol. 94, No. 10, (2011), 3249-3255.
5. Maleki-Shahraki, M., Mahmoudi, P., Abdollahi, M., Ebadzadeh, T., "Fine-grained SnO_2 varistors prepared by microwave sintering for ultra-high voltage applications", *Materials Letters*, Vol. 230, (2018), 9-11.
6. Maleki-Shahraki, M., Mahmoudi, P., Golmohammad, M., Chermahini, M.D., "Microstructural developments and electrical properties of novel coarse-grained SnO_2 varistors obtained by CuO addition for low-voltage applications", *Ceramics International*, Vol. 44, No. 15, (2018), 18478-18483.
7. Pianaro, S.A., Bueno, P.R., Longo, E., Varela, J.A., "A new SnO_2 -based varistor system", *Journal of Materials Science Letters*, Vol. 14, No. 10, (1995) 692-694.
8. Cerri, J.A., Leite, E.R., Gouvea, D., Longo, E., "Effect of cobalt(II) oxide and manganese(IV) oxide on sintering of tin(IV) oxide" *Journal of the American Ceramic Society*, Vol. 79, No. 3, (1996), 799-804.
9. Pianaro, S.A., Bueno, P.R., Longo, E., Varela, J.A., "Microstructure and electric properties of a SnO_2 based varistor", *Ceramics International*, Vol. 25, No. 1, (1999), 1-6.
10. Brankovic, G., Brankovic, Z., Davolos, M. R., Cilense, M., Varela, J. A., "Influence of the common varistor dopants (CoO , Cr_2O_3 and Nb_2O_5) on the structural properties of SnO_2 ceramics", *Materials Characterization*, Vol. 52, No. 4-5, (2004) 243-251.
11. Wang, J.F., Chen, H.C., Su, W.B., Zang, G.Z., Zhang, C.J., Wang, C.M., Qi, P., "(Gd, Co, Ta)-Doped SnO_2 Varistor Ceramics", *Journal of Electroceramics*, Vol. 14, No. 2, (2005), 133-137.
12. Qi, P., Wang, J.F., Su, W.B., Chen, H.C., Zang, G.Z., Wang, C.M., Ming, B.Q., "(Yb,Co,Nb)-doped SnO_2 varistor ceramics", *Materials Science and Engineering B*, Vol. 119, No. 1, (2005) 94-98.
13. Oliveira, M.M., Bueno, P.R., Longo, E., Varela, J.A., "Influence of La_2O_3 , Pr_2O_3 and CeO_2 on the nonlinear properties of SnO_2 multicomponent varistors", *Materials Chemistry and Physics*, Vol. 74, No. 2, (2002), 150-153.
14. Oliveira, M.M., Soares-Jr, P.C., Bueno, P.R., Leite, E.R., Longo, E., Varela, J.A., "Grain-boundary segregation and precipitates in La_2O_3 and Pr_2O_3 doped SnO_2 - CoO -based varistors", *Journal of the European Ceramic Society*, Vol. 23, No. 11, (2003) 1875-1880.
15. Wang, C.M., Wang, J.F., Su, W.B., Chen, H.C., Wang, C.L., Zhang, J.L., Zang, G.Z., Qi, P., Gai, , Ming, Q., "Improvement in the nonlinear electrical characteristics of SnO_2 ceramic varistors with Dy_2O_3 additive", *Materials Science and Engineering: B*, Vol. 127, No. 2-3, (2006) 112-116.
16. Bastami, H., Taheri-Nassaj, E., "Effect of Sm_2O_3 on the microstructure and electrical properties of SnO_2 -based varistors", *Ceramics International*, Vol. 38, No. 1, (2012), 265-270.
17. Bueno, P.R., Varela, J.A., Longo, E., " SnO_2 , ZnO and related polycrystalline compound semiconductors: An overview and review on the voltage-dependent resistance (non-ohmic) feature", *Journal of the European Ceramic Society*, Vol. 28, No. 3, (2008), 505-529.
18. Jorgensen, P.J., Westbrook, J.H., "Role of solute segregation at grain boundaries during final-stage sintering of alumina", *Journal of the American Ceramic Society*, Vol. 47, No. 7, (1964) 332-338.
19. Li, J.G., Ikegami, T., Mori, T., "Low temperature processing of dense samarium-doped CeO_2 ceramics: sintering and grain growth behaviors", *Acta Materialia*, Vol. 52, No.8, (2004) 2221-2228.
20. Upadhyaya, D.D., Bhat, R., Ramanathan, S., Roy, Schubert, S.K. H., Petzow, G., "Solute effect on grain growth in ceria ceramics", *Journal of the European Ceramic Society*, Vol. 14, No. 4(1994) 337.
21. Kingry, W.D., "Plausible concepts necessary and sufficient for interpretation of ceramic grain boundary phenomena", *Journal of the American Ceramic Society*, Vol. 57, (1974), 1-8.
22. Mendelson, M.I., "Average grain size in polycrystalline ceramics", *Journal of the American Ceramic Society*, Vol. 52, No. 8, (1969) 443-446.
23. Groza, J.R., Nanocrystalline powder consolidation methods, in: C.C. Koch (Ed.), Nanostructured materials: processing, properties, and applications, 2nd Ed., William Andrew, Inc., 2007, 173-234.
24. Rahaman, M.N., Ceramic processing and sintering, 2nd edition, theory of solid State and viscous sintering, marcel dekker Inc., New York, 2003, pp.483-486.
25. W.D. Kingery, H.K. Bowen, D.R. Uhlmann, Introduction to ceramics, 2nd edition, grain growth, sintering and vitrification, Wiley, New York, 1976, pp. 469-470.
26. Rahaman, M. N., Ceramic processing, sintering and microstructure development, Taylor and Francis, Boca Raton, London, New York, 2007, pp. 365-410.
27. Hesabi, Z.R., Mazaheri, M., Ebadzadeh, T., "Enhanced electrical conductivity of ultrafine-grained $8\text{Y}_2\text{O}_3$ stabilized ZrO_2 produced by two-step sintering technique", *Journal of Alloys and Compounds*, Vol.494, No. 1-2, (2010) 362-365.
28. S.J.L. Kang, Sintering, densification, grain growth and microstructure, grain boundary segregation and grain boundary migration, Elsevier, Oxford, 2005, 97-99.